

# Analysis of Multiple TRIGA-Based Molybdenum Production Reactor Cores Using a New Low-Enriched Uranium Target as Fuel

Andrew J. Hummel<sup>a\*</sup> and Todd S. Palmer<sup>b</sup>

<sup>a</sup>Idaho National Laboratory, Nuclear Systems Design and Analysis, 2525 Fremont Avenue, Idaho Falls, Idaho 83402

<sup>b</sup>Oregon State University, School of Nuclear Science and Engineering, Corvallis, Oregon

Received March 31, 2015

Accepted for Publication August 22, 2015

<http://dx.doi.org/10.13182/NSE15-37>

**Abstract** — The most widely used and versatile medical radioisotope today is <sup>99m</sup>Tc. Roughly 30 million people depend on this radioisotope for diagnostic imaging procedures each year, and this demand is expected to grow. Although there are numerous ways of producing this isotope, the most common is from fission product <sup>99</sup>Mo, which is produced in all nuclear reactors fueled with <sup>235</sup>U as a fission fragment with a yield of around 6.1%. Molybdenum-99 has a half-life of just over 2.5 days, and it will decay to <sup>99m</sup>Tc 87% of the time. The Reduced Enrichment for Research Test Reactors program was established at Argonne National Laboratory in 1978 to investigate technology that would aid in converting highly enriched uranium (HEU) facilities to low-enriched uranium (LEU) fuel. Since the majority of all <sup>99</sup>Mo produced currently comes from the irradiation of HEU fuel targets, there has been a growing effort to design LEU targets that can yield comparable quantities of high specific activity <sup>99</sup>Mo. Recently, a novel LEU target design has been developed for use in TRIGA reactors for the production of <sup>99</sup>Mo. The simulation tool MCNP5 was used to examine the neutronic behavior of multiple core configurations fueled solely with this new target.

**Keywords** — Molybdenum-99, low-enriched uranium, reactor analysis.

**Note** — Some figures may be in color only in the electronic version.

## I. INTRODUCTION

The most widely used and versatile medical radioisotope today is <sup>99m</sup>Tc, accounting for over 80% of all diagnostic nuclear medicine procedures in the world.<sup>1</sup> Technetium-99m is the meta-stable daughter radionuclide of <sup>99</sup>Mo, a fission product produced in all nuclear reactors. Most all <sup>99</sup>Mo produced comes from the fission of highly enriched uranium (HEU) targets containing around 93% <sup>235</sup>U. With the establishment of the Reduced Enrichment for Research Test Reactors (RERTR) program at Argonne National Laboratory (ANL), focus has shifted away from HEU targets toward low-enriched uranium (LEU) targets.

The major reason for this switch is concern over the proliferation risk of the HEU material. The amount of <sup>235</sup>U in LEU fuel is less than 20%, which means that new targets, operated in the same reactor environment, will require roughly five times as much uranium to produce comparable amounts of <sup>99</sup>Mo (Ref. 1). Currently, there is a major shortage in the production of radionuclides for medical purposes, and the Association of Imaging Producers and Equipment Suppliers (AIPES) predicts a 1.5% to 2.5% rate of growth in demand over the next 10 years.<sup>2</sup> Due to recent shortages and advances in technology, the current demand stands between 9500 and 10 000 six-day curies per week.<sup>3</sup> The motivation behind this analysis ultimately stems from the United States' inability to meet the current and expected future demand of medical

\*E-mail: [andrew.hummel@inl.gov](mailto:andrew.hummel@inl.gov)

radioisotopes (specifically  $^{99m}\text{Tc}$ ) while shifting away from HEU technology. A novel LEU target design has recently been developed at Oregon State University for the production of  $^{99}\text{Mo}$  (Ref. 4). This work analyzes the viability of operating a low-power research reactor such as the Oregon State TRIGA Reactor (OSTR) using the newly developed targets as the sole source of fissile material (standard  $\text{UZrH}_{1.6}$  fuel-followed control rods are used in these core designs).

### I.A. Motivation and Present State of $^{99}\text{Mo}$ Production

There are roughly 250 research reactors worldwide, but only nine operate on an industrial scale for medically produced radionuclides.<sup>5</sup> These include the National Research Universal (NRU) reactor in Canada, the High Flux Reactor (HFR) in the Netherlands, the Belgium Reactor 2 (BR2) in Mol, the OSIRIS reactor in France, the South African Fundamental Atomic Research Installation-I (SAFARI) reactor in South Africa, the MARIA reactor in Poland, the LVR-15 reactor in the Czech Republic, the OPAL reactor in Australia, and the RA-3 reactor in Argentina. They account for over 95% of the production of  $^{99}\text{Mo}$  and supply irradiated targets to six processing facilities: Mallinckrodt, IRE, MDS NORDION, ANSTO, NTP, and CNEA (Ref. 4). However, several of these reactors are approaching 50 years of operation, and temporary outages have caused supply problems in the past.<sup>6</sup> Unplanned shutdowns such as these put huge strains on the medical isotope market. In fact, leading experts believe that to ensure an uninterrupted  $^{99}\text{Mo}$  supply to accommodate 100% of demand, a redundancy in production capability of 250% is needed.<sup>2</sup> There are also very few new reactors slated for construction. Originally, the MAPLE I and II reactors were to be built at Chalk River Laboratories in Canada for the sole purpose of producing medical isotopes along with a New Processing Facility (NPF) to handle the irradiated targets. In June 2003, a positive coefficient of reactivity (COR) was observed in MAPLE I, and this ultimately halted operation.<sup>7</sup> The underlying cause could not be determined, and construction stopped in 2008. Operating just one of these reactors at its designed capacity would have yielded almost enough  $^{99}\text{Mo}$  to equal the worldwide demand. With the announcement of the cancelation of these two reactors, Atomic Energy of Canada, Ltd. (AECL) sought a 5-year license extension for the NRU. None of the currently operating isotope production reactors are dedicated solely (100%) to medical isotope production.<sup>8</sup> Currently seven new research reactors around the world are under construction, among which the Jules Horowitz Reactor (JHR) to be built in France (Cadarache) will be involved in  $^{99}\text{Mo}$

production.<sup>9</sup> The only reactor producing radioisotopes currently operating with both LEU fuel and targets is the OPAL reactor in Australia.

The United States has no reactors dedicated to  $^{99}\text{Mo}$  production or any processing facilities to recover the radioisotope, and the United States constitutes 50% of the market demand.<sup>10</sup> Although  $^{99}\text{Mo}$  production is an international business, one European study rightly proclaims that because “more than 50% decays away every 3 days . . . the responsibility for efficient and secure supply is more local, so in the case of Europe, the responsibility is European,” and likewise in the United States, the responsibility is our own.<sup>11</sup> The two primary sources for the United States are NRU and HFR, both of which utilize LEU fuel but HEU targets. The United States will eventually need to obtain some level of independence from foreign markets. Prior to its shutdown in 1989 due to tritium contamination, Cintichem, Inc., produced  $^{99}\text{Mo}$  at its 5-MW reactor in New York, and as of 2009, Babcock & Wilcox and the Missouri University Research Reactor (MURR) were the two leading U.S. organizations trying to produce  $^{99}\text{Mo}$  using LEU targets, although there are others such as Eden Radioisotopes.<sup>7,12</sup> The most reliable figure for the global supply and demand of  $^{99}\text{Mo}$  was estimated to be roughly 9500 to 10 000 six-day curies per week in 2012, and the United States accounts for nearly half the demand.<sup>3</sup> Our work demonstrates that operating a low-power research reactor, such as OSTR, fueled solely with the newly designed LEU targets can successfully accommodate this demand. A variety of reactor physics parameters are examined to characterize the several reactor core variations for viability and safety.

## II. OREGON STATE TRIGA REACTOR CORE DESCRIPTION

OSTR is an above-ground Mark II design, 1-MW (licensed for 1.1) natural convection cooled pool-type reactor that can operate in square-wave or pulse mode. It is strictly a research reactor and, therefore, does not generate electricity. Unlike commercial power reactors, OSTR does not operate continuously and is instead shut down at the end of each day. The core lies at the bottom of an aluminum tank roughly 2 m in diameter and 6.2 m deep. The core is nearly one-third water by volume. Nearly 5 m of water rests above the core to provide shielding at the top, and 45 cm of water, 5 cm of lead, 25 cm of graphite, and 2.5 m of concrete shield in the radial direction.<sup>13</sup> Criticality was first reached in 1967 with TRIGA standard fuel, but since 2008, the reactor has operated using LEU fuel. Altogether, 66 fuel elements were used to take the LEU core critical. A bridge atop the reactor has drives for the regulating, shim, safety, and transient control rods. The aluminum-clad transient control rod measures

about 94 cm (37 in.) and contains 38.1 cm (15 in.) of borated graphite. Unlike the other three control rods, which are driven by a motor, the transient rod is pneumatically controlled.

Six concentric rings (referred to as B through G, A being the center position) hold the 126 spaces for the fuel rod elements, control rods, guide tubes, and pneumatic transfer tube as shown in Fig. 1. Each tube measures approximately 3.8 cm in diameter. A roughly 2-cm (3/4-in.) aluminum grid plate sits at the bottom to support the core and receives the adaptor ends of the fuel/moderator elements and pneumatic transfer tube. Another aluminum plate sits at the top and allows for accurate positioning of the different core components. The current LEU fuel is a homogeneous mixture of uranium and zirconium hydride,  $\text{UZrH}_{1.6}$ , and measures approximately 38.1 cm (15 in.) in length. The core consists of these fuel elements and dummy aluminum-clad graphite elements along with the AmBe source located in the G17 position and various irradiation facilities.

The LEU target designed by Oregon State University and researchers from Pacific Northwest National Laboratory consists of 19.75%  $\text{UO}_2$  sandwiched between two aluminum cylinders. The actual fuel targets are annular in design, which

allows the water moderator/coolant to flow through the center of the targets and greatly increases the thermalization of neutrons. This has the benefit of reducing the self-shielding in the fuel, which will ultimately lead to an increase in the utilization of the fuel. Also, the annulus almost doubles the surface area between the fuel target and coolant, leading to an increase in the heat transfer capabilities. Although the fabrication and design specifics of this target are proprietary, the dimensions given in Table I are sufficient to model the

TABLE I  
LEU Target Dimensions

Central water radius	1.33096 cm
Inner-aluminum-clad outer radius	1.48844 cm
Fuel outer radius	1.71577 cm
Outer-aluminum-clad outer radius	1.87579 cm
Active fuel length	48.0065 cm
Top air follower region	5.3335 cm
Top aluminum cap	2.31 cm
$\text{UO}_2$ volume/target	109.857 $\text{cm}^3$
$^{235}\text{U}$ mass/target	~158 g

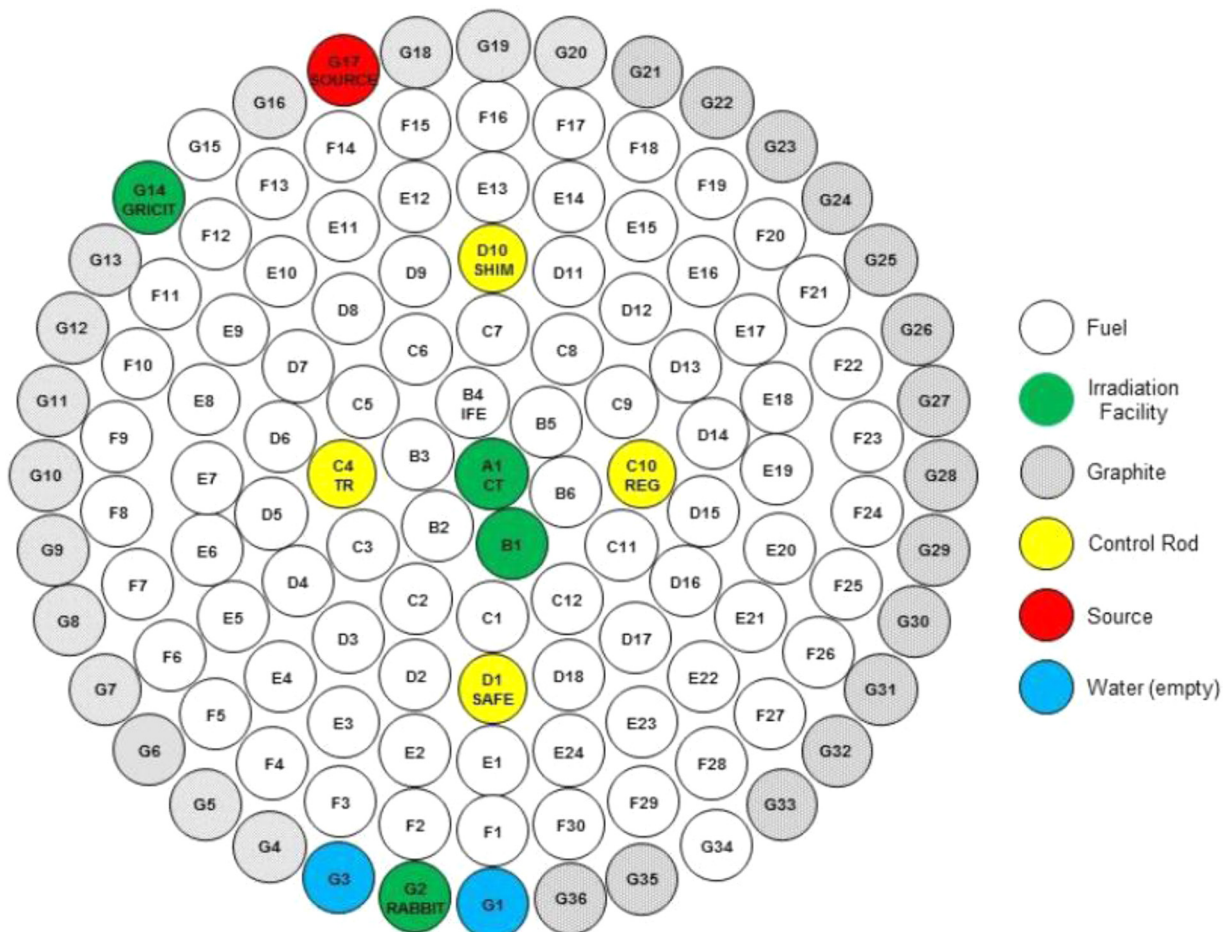


Fig. 1. Radial view of OSTR.

target and perform the necessary analysis. Figure 2 shows an axial view of the target.

### III. RESULTS

During the conversion of the OSTR to LEU fuel in 2008, an MCNP5 model of the core was developed and was subsequently benchmarked after refueling. Extensive measurements have been performed to verify its predictions.<sup>14,15</sup> The nuclear data library used for this work is ENDF.60c, which corresponds to a temperature of 293.6 K. The behavior of the core containing only the new LEU targets (and dummy graphite reflector elements) was first examined by replacing all 87 fuel elements. Reactivity coefficients compared well with the LEU normal core, but the core failed to have sufficient negative reactivity to shut down. We, therefore, focused on smaller cores, still with no driver assemblies (nontarget fuel). The two general core layouts analyzed were: (1) loading the inner B, C, and D rings with target elements (the three-ring core) and (2) loading the inner B, C, D, and E rings with target elements (the four-ring core). All nontarget filled positions contain graphite reflector elements (except those that contain control rods and the source). As licensed, the OSTR can accommodate up to nine control rods, five more than are present in its current operational configuration, and these positions are fixed. The additional control rods were modeled as both fuel-followed and air-followed. The three variants of the smaller core that were analyzed each contain 32 LEU targets filling the B, C, and D rings. The larger four-ring core was examined with 52, 54, and 56 LEU targets. However, the cores with 56 targets did not have sufficient negative reactivity to shut down, and the results will, therefore, not be presented. The standard four control rods lie in the C4, C10, D1, and D10 positions. Position A1 can potentially contain a control rod; thus, it was modeled as an aluminum slug (current design), a fuel-followed control rod (FFCR),

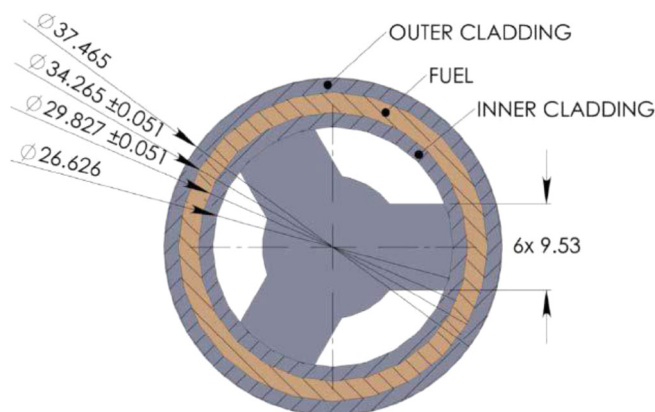


Fig. 2. Radial view of LEU target.

and an air-followed control rod (AFCR). In the four-ring cores, positions D12, D17, E4, and E9 were also modeled as FFCRs and AFCRs. The FFCRs contain standard LEU TRIGA fuel ( $\text{U}\text{ZrH}_{1.6}$ ) as the following material.

#### III.A. Power Profile

Figures 3, 4, and 5 illustrate the general power profile across the different cores in kilowatts per pin. The power is normalized in MCNP5 to 1.1 MW(thermal). This includes the power generated in the FFCRs.

The power decreases radially out from the center of the cores, and the hottest pin occurs at the B3 position for all cores examined, which is in line with normal operation of the OSTR with LEU fuel. The maximum pin power observed is 36.21 kW. All control rods are withdrawn such that the center position is either aluminum, air, or  $\text{U}\text{ZrH}_{1.6}$  fuel. Because the power is limited to a maximum of 1.1 MW and normalized over all fission (power) generating elements, the power generated per pin in the three-ring core with aluminum or air occupying the A1 position will be greater than in the cores with FFCRs. Aluminum compared to air will lead to a slight increase in the thermalization in the center of the core since the neutrons basically stream unabated through air. However, the neutron absorption cross section of aluminum is much higher than that of air, and this should help to flatten the flux profile across the core. The peak-to-average power ratio is approximately 1.17 for the three-ring cores and 1.26 in the four-ring cores. Since power is generated in the FFCRs, the cores with AFCRs have a slightly higher average pin power.

#### III.B. Molybdenum-99 Production

The production of  $^{99}\text{Mo}$  for the different viable cores is shown in Table II and is directly proportional to the power level. The cores yield slightly higher quantities of  $^{99}\text{Mo}$  when they contain AFCRs rather than FFCRs for a given irradiation time. Again, this is because the 1.1 MW(thermal) maximum power is normalized over all power-generating elements, and those cores with FFCRs contain more of these elements. All seven cores yield  $^{99}\text{Mo}$  production activities that far exceed the U.S. weekly demand of ~6000 six-day curies. For both the three-ring and four-ring cores, the number of curies of  $^{99}\text{Mo}$  produced as a function of Mo mass (specific activity or SA) and  $^{235}\text{U}$  mass is virtually the same given a constant irradiation time. This is to be expected since the power is normalized to the same constant (1.1 MW), the molybdenum isotopes are bred into the reactor at a constant rate, and the isotope decays at a constant rate.

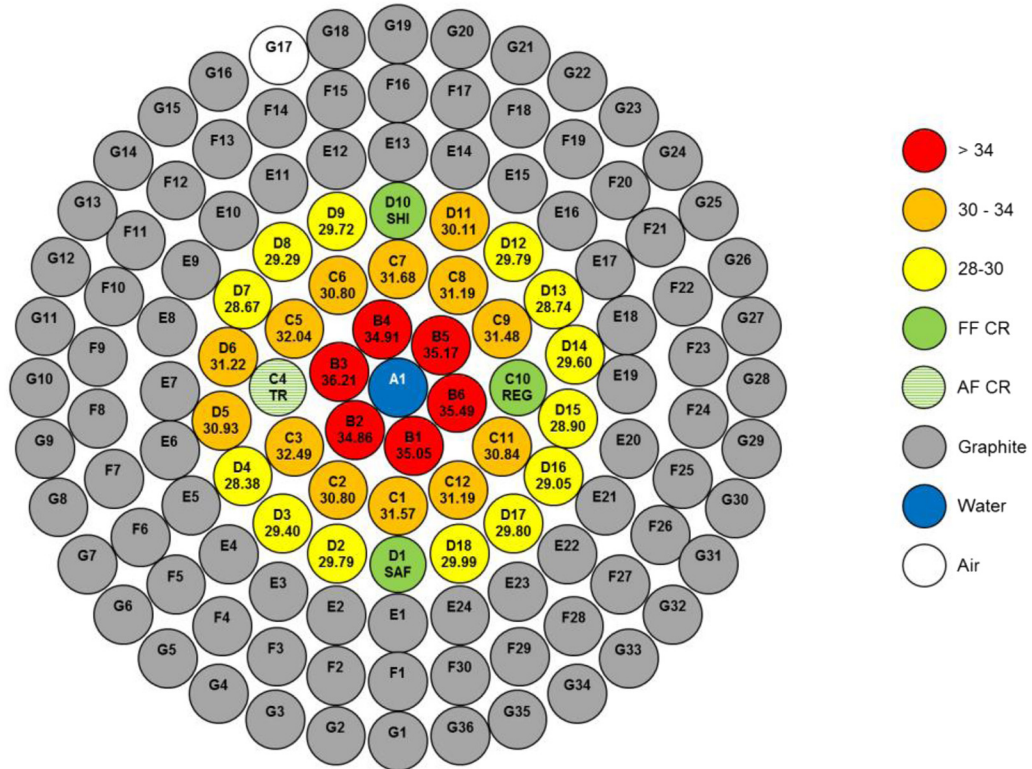


Fig. 3. Typical power profile across the three-ring core (no additional control rods).

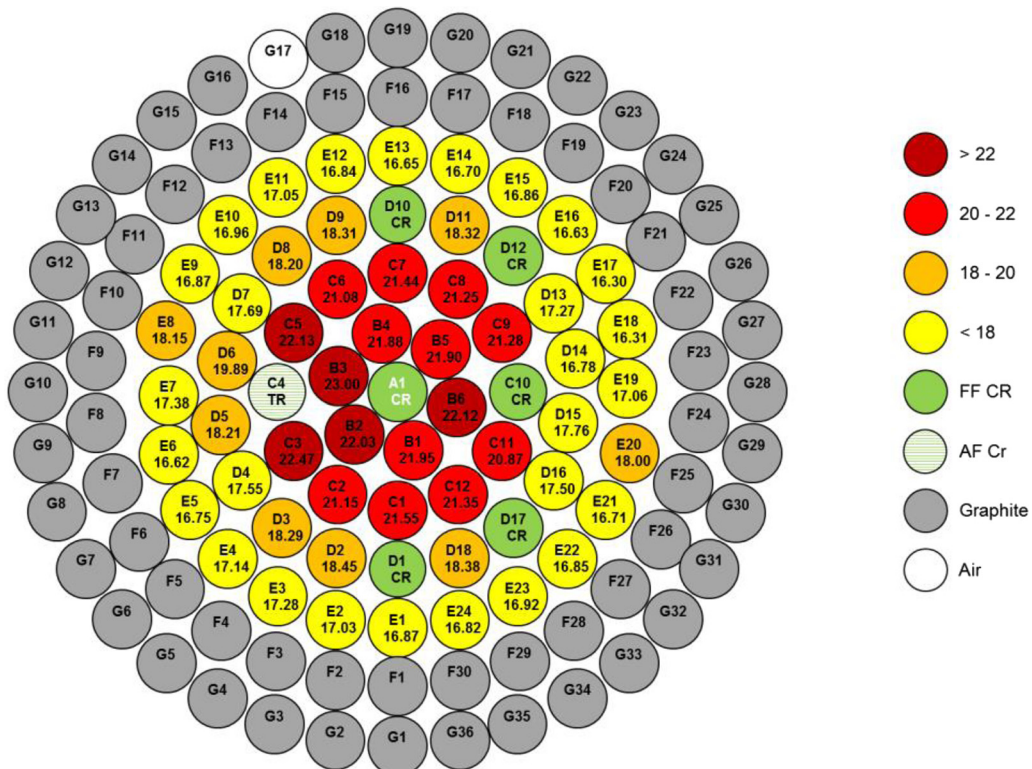


Fig. 4. Typical power profile across the four-ring core with 54 targets (two additional control rods).

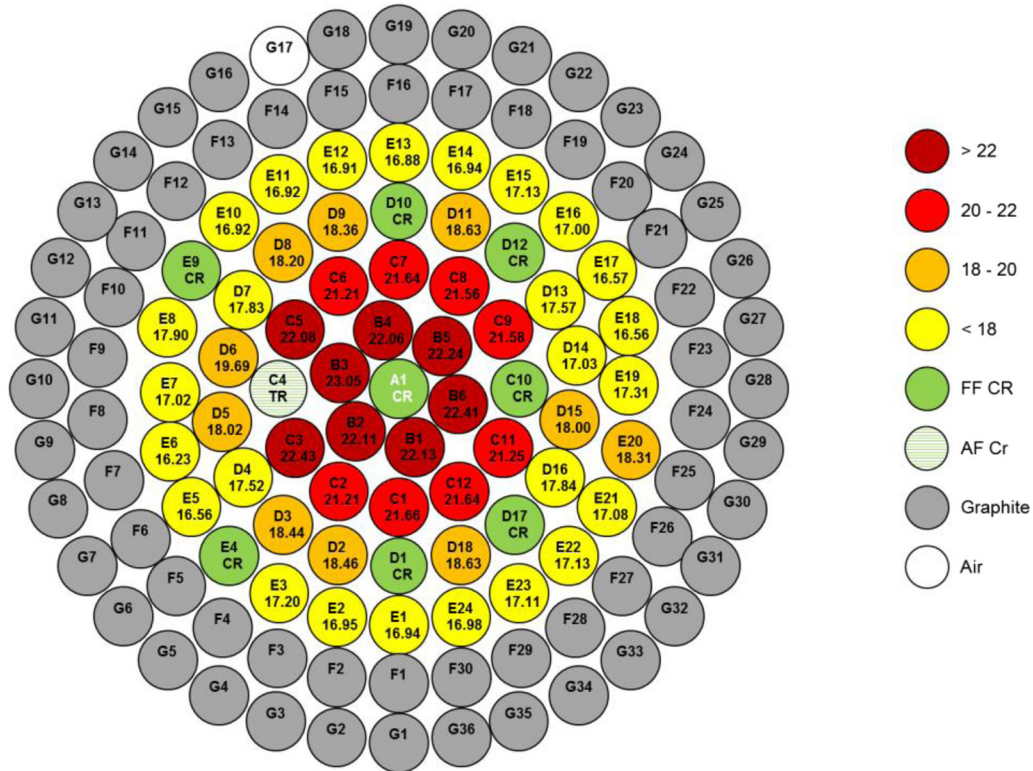


Fig. 5. Typical power profile across the four-ring core with 52 targets (four additional control rods).

TABLE II  
Molybdenum-99 Production After 5 and 7 Days of Irradiation

Core	Irradiation Time (days)	Total		Average per Target			
		<sup>99</sup> Mo Activity (10 <sup>4</sup> Ci)	6-Day Ci (10 <sup>3</sup> )	<sup>99</sup> Mo Activity (10 <sup>3</sup> Ci)	6-Day Ci	6-Day SA (Ci <sup>99</sup> Mo/mg Mo)	Ci <sup>99</sup> Mo/g <sup>235</sup> U
3-ring: A1 slug	5	4.09	7.00	1.28	219	13.3	8.09
	7	4.73	8.09	1.48	253	11.3	9.36
3-ring: A1 FFCR	5	4.00	6.84	1.25	214	13.3	7.92
	7	4.63	7.92	1.45	248	11.3	9.16
3-ring: A1 AFCR	5	4.08	6.98	1.28	219	13.3	8.08
	7	4.72	8.07	1.48	253	11.3	9.34
4-ring: A1, D12, D17 FFCR	5	4.12	7.05	0.764	131	13.3	4.83
	7	4.77	8.16	0.883	151	11.3	5.59
4-ring: A1, D12, D17 AFCR	5	4.31	7.37	0.799	137	13.3	5.06
	7	4.99	8.53	0.924	158	11.3	5.85
4-ring: A1, D12, D17, E4, E9 FFCR	5	4.01	6.86	0.771	132	13.3	4.88
	7	4.64	7.94	0.892	153	11.3	5.65
4-ring: A1, D12, D17, E4, E9 AFCR	5	4.31	7.37	0.828	142	13.3	5.24
	7	4.98	8.52	0.958	164	11.3	6.06

### III.C. Reactor Physics Parameters

The delayed neutron fraction, mean neutron lifetime, moderator COR, and void COR for the analyzed cores are

shown in Table III. Also included are these quantities for the OSTR in normal operation mode and the TRIGA at Reed College, both utilizing the standard LEU UZrH<sub>1.6</sub> fuel.<sup>13,16</sup> The delayed neutron fractions for the <sup>99</sup>Mo target

TABLE III  
Reactivity Coefficients, Delayed Neutron Fraction, and Mean Neutron Lifetime

Core	Delayed Neutron Fraction	Mean Neutron Lifetime ( $\mu\text{s}$ )	Moderator COR ( $\text{¢}/^\circ\text{C}$ )	Void COR ( $\text{\$/\% void}$ )
3-ring: A1 slug	$0.00737 \pm 0.0003$	$18.9 \pm 5.9$	$-1.82 \pm 0.1$	$-1.73 \pm 0.07$
3-ring: A1 FFCR	$0.00742 \pm 0.0002$	$38.5 \pm 5.5$	$-1.79 \pm 0.1$	$-1.74 \pm 0.08$
3-ring: A1 AFCR	$0.00739 \pm 0.0002$	$26.0 \pm 5.5$	$-1.89 \pm 0.1$	$-1.77 \pm 0.05$
4-ring: A1, D12, D17 FFCR	$0.00729 \pm 0.0002$	$31.9 \pm 4.4$	$-1.17 \pm 0.09$	$-1.18 \pm 0.03$
4-ring: A1, D12, D17 AFCR	$0.00670 \pm 0.0002$	$23.2 \pm 4.6$	$-1.75 \pm 0.1$	$-1.31 \pm 0.03$
4-ring: A1, D12, D17, E4, E9 FFCR	$0.00717 \pm 0.0003$	$32.3 \pm 4.6$	$-1.37 \pm 0.1$	$-1.24 \pm 0.03$
4-ring: A1, D12, D17, E4, E9 AFCR	$0.00637 \pm 0.0003$	—	$-1.58 \pm 0.1$	$-1.48 \pm 0.04$
OSTR normal beginning of life	0.0076	22.6	-0.72	-0.96
Reed TRIGA (Ref. 17)	0.00778	—	-0.5688	-0.8300

fueled cores are lower than the normal OSTR core and the TRIGA at Reed. The mean neutron lifetime is longer for the FFCR cores as opposed to the AFCR cores. Since the air basically represents a void, neutrons will stream through these regions, and if they are traveling in an axial direction, they are much more likely to escape from the core.

The cores containing similar numbers of targets had virtually identical reactivity coefficients, and the averages of these values are shown graphically. Figure 6 shows the moderator temperature COR for the different cores over the temperature intervals from 20°C to 40°C, 40°C to 60°C, and 20°C to 60°C with uncertainties given in the Appendix. The COR was determined by changing the density of the moderator associated with these temperatures. This approach was used in the analyses of the converted LEU core for the OSTR and utilizes the ENDF-VI evaluated nuclear cross-section data for these temperatures. As the moderator temperature increases, which corresponds to a decrease in density, all cores show an increase in the negative reactivity insertion that is about 2.5 to 3 times greater than the OSTR normal core and Reed TRIGA. This

COR is plotted at the midpoint of these temperature ranges. The prompt fuel temperature COR was determined over four temperature ranges and is plotted at the midpoint of each temperature interval in Fig. 7. Unlike the standard  $\text{UZrH}_{1.6}$  fuel, the fuel temperature COR for the  $\text{UO}_2$  targets becomes less negative as the fuel temperature increases. Nonetheless, it does remain negative over the range of 293 to 2500 K.

A comparable analysis can be made for the void COR. This quantity is given in units of  $\text{\$/\%}$  of the core voided. The change of reactivity  $\rho$  is calculated by comparing the core multiplication computed with the innermost channel in a completely voided state to that in which it is 10% voided. The volume of the moderator in the innermost channel of the core represents approximately 12.2%, 8.2%, 5.90%, and 8.20% of the total moderator volume in the three-ring cores, four-ring cores, the normal OSTR, and the Reed TRIGA, respectively. Although the voided region is a greater percentage by volume for the three-ring cores, the loss in reactivity due to the void in the moderator outweighs the difference in volume, providing a strong negative feedback mechanism. Figure 8

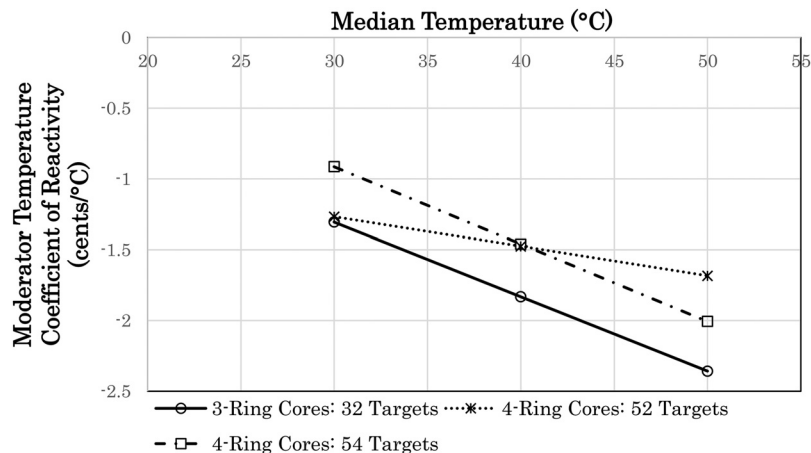


Fig. 6. Moderator temperature COR plotted at the midpoint temperature range.

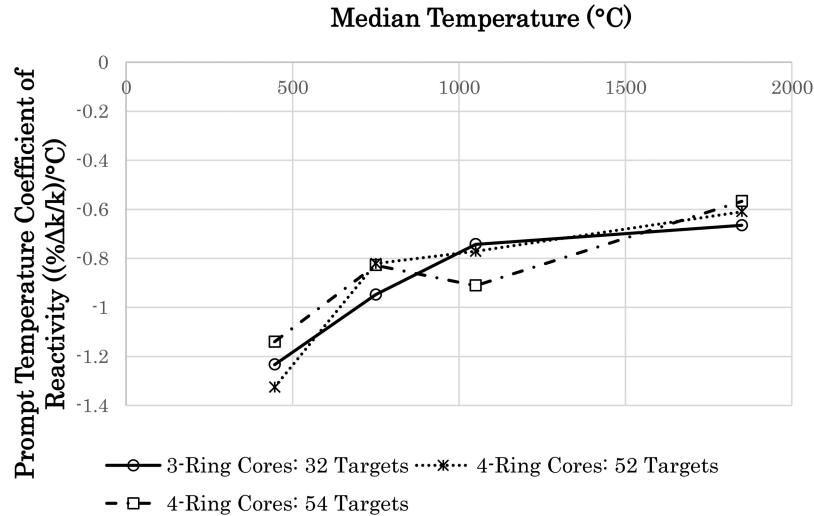


Fig. 7. Prompt fuel temperature COR plotted at the midpoint temperature range.

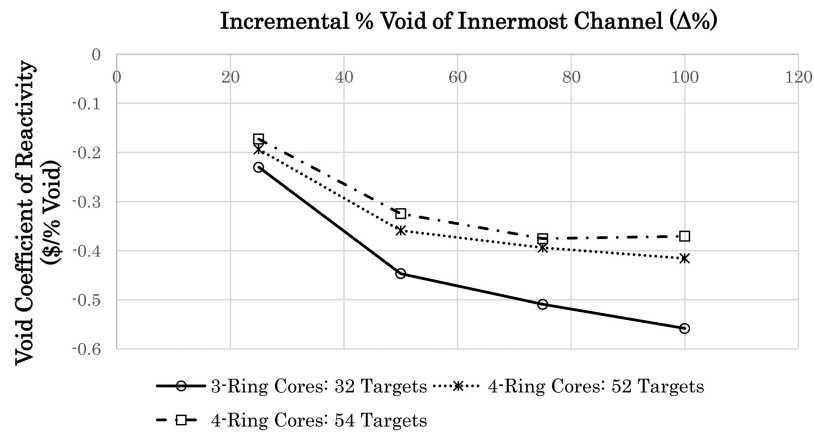


Fig. 8. Void COR between 10% and 25%, 25% and 50%, 50% and 75%, and 75% and 100% plotted at the high end.

shows the void COR as the void in the innermost channel incrementally increases from 10% to 25%, 25% to 50%, 50% to 75%, and 75% to 100% with the COR graphed at the high end of these ranges. Figure 9 shows the void COR as the void range increases from 75% to 100%, 50% to 100%, 25% to 100%, and 10% to 100% (i.e., 25%, 50%, 75%, and 90% increases in the void) and is graphed compared to the percentage difference. For all cores, as the void increases, there is an increase in the negative reactivity insertion. This is expected, as there will be a strong decrease in the moderation. All cores examined have a roughly 1.5- to 2-fold increase in negative reactivity compared to the OSTR normal core and Reed TRIGA.

All CORs should be negative and this is what is observed. As the moderator temperature increases, the neutron spectrum shifts to higher energies, increasing the resonance absorption. The more profound effect results from the decrease in thermalization as the density of water decreases. Since the targets allow water to flow through the annulus,

these cores are much more responsive to changes in the moderator density than standard TRIGA cores with solid  $UZrH_{1.6}$  fuel, providing a valuable negative feedback mechanism. Unlike standard TRIGA LEU fuel, the prompt fuel temperature COR does not become more negative as the temperature increases (although it does remain negative). This is an inherent feature of  $UZrH_{1.6}$  fuel and one of the reasons that TRIGA reactors are capable of pulsing. The  $^{99}Mo$  target fueled cores would not be operated in pulse mode.

The total rod worth, excess reactivity, and shutdown margin were calculated by comparing the core multiplication factors with the control rods completely withdrawn and fully inserted. For an accident involving one of the control rods becoming stuck out of the core and no longer available for insertion, the shutdown margin was also calculated with the most reactive rod withdrawn. The regulatory rod is the most reactive rod and is modeled as withdrawn for each core. These results are shown in Table IV. These values satisfy the current limits of the OSTR operational license.

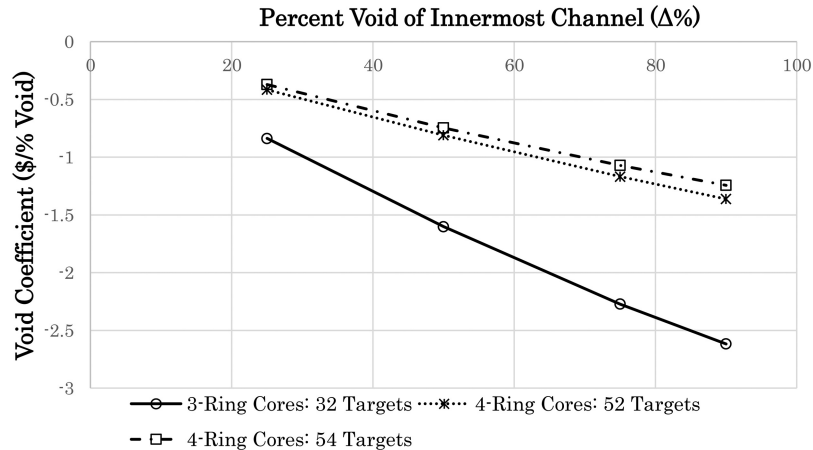


Fig. 9. Void COR between 75% and 100%, 50% and 100%, 25% and 100%, and 10% and 100%.

TABLE IV

Reactor Physics Parameters

Core	Total Rod Worth (\$)	Excess Reactivity (\$)	Shutdown Margin (\$)	Shutdown Margin with Regulatory Rod Out (\$)
3-ring: A1 slug	18.2 ± 0.62	2.33 ± 0.080	15.9 ± 0.54	8.79 ± 0.30
3-ring: A1 FFCR	26.6 ± 1.1	2.80 ± 0.12	23.8 ± 1.0	16.4 ± 0.70
3-ring: A1 AFCR	26.7 ± 1.1	2.00 ± 0.083	24.3 ± 1.0	16.8 ± 0.69
4-ring: A1, D12, D17 FFCR	22.4 ± 0.78	16.3 ± 0.55	6.06 ± 0.21	2.53 ± 0.086
4-ring: A1, D12, D17 AFCR	22.0 ± 0.90	15.3 ± 0.56	6.74 ± 0.25	3.34 ± 0.12
4-ring: A1, D12, D17, E4, E9 FFCR	27.8 ± 1.0	15.9 ± 0.56	12.0 ± 0.42	7.41 ± 0.26
4-ring: A1, D12, D17, E4, E9 AFCR	27.2 ± 1.3	13.9 ± 0.57	13.3 ± 0.55	9.51 ± 0.39
OSTR beginning of life	11.37 ± 0.33	5.48 ± 0.012	—	1.21 ± 0.04

## IV. CONCLUSIONS

The OSTR was used as the design basis for the  $^{99}\text{Mo}$  cores examined, and the MCNP5 simulation package was utilized to perform this analysis. Both the normal OSTR core and the target fueled  $^{99}\text{Mo}$  cores examined are fueled with LEU. The two primary differences in the fuel and targets are the composition and design. The normal OSTR core uses  $\text{UZrH}_{1.6}$  as the fuel material while the  $^{99}\text{Mo}$  cores utilize  $\text{UO}_2$ , which acts as both the fuel and target material. The annular design of the targets allows the coolant/moderator to flow through the center of the  $^{99}\text{Mo}$  targets, whereas the  $\text{UZrH}_{1.6}$  fuel design does not. The normal OSTR core contains 87 fuel elements that are designed to last for the operational lifetime of the OSTR. The  $^{99}\text{Mo}$  cores examined contain 32 targets, making the  $^{99}\text{Mo}$  cores much smaller than the normal OSTR core, and these targets will be processed after a 5- to 7-day irradiation cycle. Additional control rods were examined in the  $^{99}\text{Mo}$  cores to control the reactivity present. The additional air-followed and

fuel-followed control rods examined are identical in design to the current control rods in the core.

All three designs yield well over the roughly 6000 six-day curie weekly U.S. demand after 5 days of irradiation and these results compare well with those found in the literature for other  $^{99}\text{Mo}$  production research reactors.<sup>17,18</sup> All CORs are negative and all three cores have sufficient shutdown margins with the regulating rod stuck out of the core.

## V. FUTURE AND ONGOING WORK

Other core designs have been examined, and the results from those will be presented later. There is ongoing work using ORIGEN-ARP to quantify the SA in the targets better. Due to the high pin power, it may be necessary to use RELAP5-3D to determine the minimum critical heat flux ratio (MCHFR). A prior study of the LEU  $\text{UZrH}_{1.6}$  fuel determined the MCHFR to be approximately 1 at 35 kW, and a more recent analysis of the  $\text{UO}_2$  targets analyzed pin powers up to 20 kW (Refs. 19 and 20). Based on these studies, the high pin power in the  $\text{UO}_2$  targets does not

appear to be a problem, yet further analysis may be needed to determine the MCHFR more accurately.

**APPENDIX**

The moderator COR error, void COR error, and prompt fuel temperature COR error can be found in Tables A.I, A.II, and A.III, respectively.

**Acknowledgments**

The authors wish to thank the Oregon State University Radiation Center director, S. Reese, and reactor administrator, S. T. Keller, for their assistance with TRIGA reactor operational data and dimensions. The authors also thank reactor physicist R. Schickler.

**References**

1. “Production Technologies for Molybdenum-99 and Technetium-99m,” IAEA-TECDOC-1065, International Atomic Energy Agency (1999).
2. P. VERBEEK, “Report on Molybdenum-99 Production for Nuclear Medicine 2010–2020,” Association of Imaging Producers & Equipment Suppliers, European Industrial

Association for Nuclear Medicine and Molecular Healthcare (2008).

3. “A Supply and Demand Update of the Molybdenum-99 Market,” Organisation for Economic Co-operation and Development/Nuclear Energy Agency (2012); <https://www.oecd-nea.org/med-radio/docs/2012-supply-demand.pdf> (current as of Mar. 31, 2015).
4. W. R. MARCUM, P. Y. BYFIELD, and S. R. REESE, “A New Molybdenum Production Element for Implementation in TRIGA Reactors: Thermal-Hydraulic Characterization,” *Nucl. Sci. Eng.*, **180**, 2, 123 (2015); <http://dx.doi.org/10.13182/NSE14-93>.
5. B. PONSARD, “Status and Future of Mo-99 Supply,” *Proc. 19th Int. Topl. Mtg. Research Reactor Fuel Management (RRFM-2015)*, Bucharest, Romania, April 19–23, 2015, p. 371, European Nuclear Society (2015).
6. S. MARCK, A. KONING, and K. CHARLTON, “The Options for the Future Production of the Medical Isotope Mo-99,” *Eur. J. Nucl. Med. Mol. Imaging*, **37**, 1817 (2010); <http://dx.doi.org/10.1007/s00259-010-1500-7>.
7. *Medical Isotope Production Without Highly Enriched Uranium*, National Academy of Sciences (2009); <http://dx.doi.org/10.17226/12569>.
8. D. LEWIS, “Mo-99 Supply—The Times They Are A-Changing,” *Eur. J. Nucl. Med. Mol. Imaging*, **36**, 1371 (2009); <http://dx.doi.org/10.1007/s00259-009-1171-4>.
9. “The Jules Horowitz Reactor : General Description,” Commissariat à l’Energie Atomique (2009); [www.cad.cea.fr/rjh/general-description.html](http://www.cad.cea.fr/rjh/general-description.html) (current as of Mar. 31, 2015).
10. S. MIRZADEH et al., “Production Capabilities in U.S. Nuclear Reactors for Medical Radioisotopes,” ORNL/TM-12010, Oak Ridge National Laboratory (1992).

TABLE A.I

Moderator COR Error

Core	20° to 40°	40° to 60°	20° to 60°
A1 slug	0.222	0.225	0.127
A1 FFCR	0.224	0.242	0.130
A1 AFCR	0.221	0.231	0.118

TABLE A.II

Void COR Error

Core	10% to 25%	25% to 50%	50% to 75%	75% to 100%	50% to 100%	25% to 100%	10% to 100%
A1 slug	0.0439	0.0418	0.0417	0.0417	0.0411	0.0410	0.0410
A1 FFCR	0.0472	0.0450	0.0449	0.0448	0.0443	0.0443	0.0442
A1 AFCR	0.0303	0.0273	0.0271	0.0270	0.0262	0.0261	0.0260

TABLE A.III

Prompt Fuel Temperature COR Error

Core	173.5°	477°	777°	1577°
A1 slug	$9.8 \times 10^5$	$1.03 \times 10^4$	$1.04 \times 10^4$	$2.40 \times 10^4$
A1 FFCR	$1.02 \times 10^4$	$1.03 \times 10^4$	$1.03 \times 10^4$	$2.57 \times 10^5$
A1 AFCR	$1.10 \times 10^4$	$1.10 \times 10^4$	$1.02 \times 10^4$	$2.57 \times 10^5$

11. A. ALBERMAN et al., “Scenario for Sustainable Molybdenum-99 Production in Europe,” European Research Reactor Position Paper, CEA, IRN, NRG, RCR, SCK-CEN, POLATOM, and TUM (2011).
12. M. VERNON, “Mo-99 Production Utilizing Target-Only Reactor Design,” *Proc. 2013 Topl. Mtg. Molybdenum-99 Technological Development*, Chicago, Illinois, 2013.
13. “Oregon State University TRIGA Reactor Safety and Analysis Report,” Chapter 4, “Oregon State TRIGA Reactor,” Oregon State University.
14. M. HARTMAN et al., “Neutronic Analysis of the Oregon State TRIGA Reactor in Support of Conversion from HEU Fuel to LEU Fuel,” *Nucl. Sci. Eng.*, **174**, 135 (2013); <http://dx.doi.org/10.13182/NSE12-5>.
15. X-5 MONTE CARLO TEAM, “MCNP—A General Monte Carlo N-Particle Transport Code, Version 5, Volume 1: Overview and Theory,” Los Alamos National Laboratory (2003).
16. S. FRANTZ, “Reed College Research Reactor License No. R-112 Docket No. 50-288,” Responses to the Request for Additional Information (2011).
17. B. PONSARD, “Production of Radioisotopes in the BR2 High-Flux Reactor for Applications in Nuclear Medicine and Industry,” *J. Labelled Compd. Radiopharm.*, **50**, 333 (2007); <http://dx.doi.org/10.1002/jlcr.1377>.
18. S. MO, “Production of Mo-99 Using LEU and Molybdenum Targets in a 1 MW TRIGA Reactor,” *Proc. Int. Mtg. Reduced Enrichment for Research and Test Reactors*, Oarai, Ibaraki, Japan, October 3–7, 1993.
19. W. R. MARCUM et al., “Steady-State Thermal-Hydraulic Analysis of the Oregon State University TRIGA Reactor Using RELAP5-3D,” *Nucl. Sci. Eng.*, **162**, 261 (2009); <http://dx.doi.org/10.13182/NSE08-63>.
20. P. BYFIELD, “A Thermal Hydraulics Analysis of a Molybdenum Production Element for Implementation in TRIGA Reactors,” MS Thesis, Oregon State University (2013).